Sample orientation and high temperature performance of T23 and T347HFG steels in steam oxidation

T. Dudziak*, M. Lukaszewicz, N. J. Simms, J. R. Nicholls**

Centre for Energy and Resource Technology
Cranfield University
Cranfield, Bedfordshire
MK43 0AL, United Kingdom

*Foundry Research Institute
Centre for High Temperature Studies
Zakopiańska 73
30-418 Kraków
Poland

** Currently at:
National Physics Laboratory
Hampton Rd, Teddington, Middlesex
TW11 0LW, United Kingdom

Abstract

Steam oxidation of candidate alloys considered for use in the Ultra Supercritical (USC) boilers is of growing interest. Ferritic (T23) and austenitic (T347HFG) steels have been studied with an emphasis on understanding the impact of temperature, chromium content and specimen geometry on their steam oxidation behaviour. Selected materials were tested at four temperatures (600 ^{o}C, 650 ^{o}C, 700 ^{o}C and 750 ^{o}C) in 100% steam conditions for 1000 hours (four cycles for 250 hours). Tests indicated that the curved-shaped specimens show slower mass gain ,scale ticking and void nucleation rates than "bridge-shaped" specimens (with flat and convex surfaces combined). The shape factor also has an impact on the scale morphology, especially on the development of the outer most haematite layer on T23 specimens in the temperature range between 600 ^{o}C and 700 ^{o}C, with the amount decreasing with increasing temperature. In comparison the T347HFG shows relatively good oxidation resistance in steam even at 750 ^{o}C for the test duration (1000 hours).

Keywords: steam oxidation; steels, oxide scale, SEM, EDX

1. Introduction

Steam oxidation is matter of growing interest as research for improvements in power plant efficiencies indicates the needs for higher temperatures and pressures [1, 2, 3] Viswanathan and Bakker et al. [2] studied topic of increasing the energy efficiency in the worldwide power plants. They indicated that since the energy crisis in 1970, the energy steam temperature for new power plants increased by about 60 ^{o}C corresponding to rise of about 6 % in energy efficiency. Moreover the steam temperature in the conventional power plant is expected to raise about 50 ^{o}C to 100 ^{o}C by 2030. Currently most of the coal-fired power plants operate at temperature between 520 ^{o}C – 565 ^{o}C and 243 bar which allows achieving efficiency of 38 - 40%.

In the new design units the efficiency of energy generation is above 40% due to higher steam conditions (600 ^{o}C – 620 ^{o}C). The most efficient power plants, which are currently designed and tested, are expected to have 44 - 46% efficiency with steam conditions of at 700 ^{o}C – 720 ^{o}C and 365 - 385 bar pressure. Using those operating conditions with traditional heat exchangers materials will lead to the development of the thick non-protective oxides and finally to component failures [4, 5, 6]. High temperature oxidation is enhanced in steam environments, therefore the materials needed for the superheater and reheater (SH/RH) tubing have to show slow oxidation rates in steam as well as good high temperature creep resistance.

The consequences of fast oxide growth are of concern due to tube overheating, scale spalling, tube blockages and steam turbine corrosion and erosion [7]. To mitigate these problems research has to be carried out to understand the influence of alloy composition, microstructure and additionally the impact of time, temperature and operational conditions [8, 9] on the materials resistance. Due to the severity of proposed operational conditions (temperatures and pressures) and the required lifetime at elevated temperature, the materials used for the Ultra Supercritical (USC) applications have to exhibit very good mechanical, physical and chemical properties [2, 7]. Among these oxidation and creep rapture resistance are believed to be of crucial importance [7]. There are three groups of alloys which could be successfully employed for the coal–fired boiler elements: ferritic, austenitic and nickel-based; however, their applications are limited up to 620 ^{o}C, 700 ^{o}C respectively [10]. Due to limited data on nickel-based alloy there is no limit identified for their application, however it is proposed that for all application above 700 ^{o}C those materials should be used [11]. High temperature oxidation in 100 % steam is characterised by faster oxidation rates than in dry or

humid environments; moreover the scale formed exhibits different adherence and porosity [12].

Both oxidation kinetics and the scale morphology are reported to be strongly dependent on the alloy composition, surface finish and test conditions: metal temperature, steam flow and chemistry [13]. Among highlighted factors of chromium level is of crucial importance [14]; however it seems to have less impact below 570 ^{o}C. Therefore for components operating at temperatures below 570 ^{o}C the steels with lower Cr levels may be employed [15]. Viswanathan et al.[7] believes that chromium content has less impact on oxidation of 9 – 12 % Cr ferritic steels below 600 ^{o}C.

Nevertheless there is no agreement on the impact of chromium on steam oxidation at different temperatures, but it is well recognised that steels with higher chromium level exhibits better oxidation resistance due to formation of more protective Cr rich oxides. However, there is no clear evidence for the minimum Cr content which is sufficient for the development of the protective chromium oxides. Shibli and Starr et. al [16] indicated that in temperature range between 600 ^{o}C – 650 ^{o}C 10 - 11 % of chromium in the base metal allows protective, external chromia (Cr_2O_3) to be formed; in contrast Sanchez et al. [14] have shown that such an oxide forming with Cr content greater than 11 – 12 % for steels exposed to steam at temperatures above 600 ^{o}C. Quadakkers et al. [17] concluded that the scale formed on ferritic and austenitic steels differs with the chromium content in the base material; it is recognised that scale changes in following manner: with increasing Cr content it changes from hematite/magnetite to magnetite/$(Fe, Cr)_3O_4$ spinel to $(Fe, Cr)_3O_4$ spinel/Cr_2O_3 and finally to a pure Cr_2O_3. Viswanathan et al. [7] proposed following ranking of the high temperature resistant alloys, due to their chromium levels and their relation with protective properties of the scale: Incaloy 740, Alloy 230, HR120, HR6W, HR3C, T347HFG, Super 304H, T92, T91 and T23.

The scales formed on the high temperature resistant alloys differ with alloy type; this is clearly associated with the chromium level as presented above, additionally the alloy structure and grain size are reported to have considerable impact [6]. Oxides developed on the ferritic steels have a duplex structure [12], inner layer with protective chromium oxides and outer with magnetite as the main constituent [7]. Although expected, the continuous layer of haematite is not always present as the outermost layer. Often there are traces of Fe_2O_3 on the surface of magnetite however it is discontinuous. Haematite is believed to form due to reduced iron diffusion through the magnetite. The slower diffusion is result of the gap nucleation between inner and outer layers or within the outer Fe_3O_4. The double-layered scale

was also found on the austenitic steels, with (Fe, Cr) spinel (inner layer) and magnetite (outer layer) as the main constituents [6], however such scale forms after long term exposure. Viswanathan et al. [7] and Hansson et al. [6] indicated that scale formed on the austenitic alloys changes with temperature; below 585 ^{o}C it shows irregular structure with some porosity, above that temperature the scale seems to be more homogenous [6]. To summarise, the main difference between the scales formed on the ferritic and austenitic steels are their properties – uniformity, thickness, porosity and adherence [4, 5 ,18].

In the present work, the steam oxidation behaviour of T23, T347HFG in a 100% steam environment will be analysed and compared. The main emphasis is on the difference between the oxides' scales developed on the investigated alloys and influence of the specimen geometry, chromium level and exposure conditions. Specimen geometry was expected to have a general impact on the oxidation process; however, its influence could be greater on the morphology of scale and spallation than process kinetics. Furthermore, the paper aims to fulfil the gap in the study of the T347HFG behaviour during short exposure time and to increase understanding of the oxidation of the austenitic steel during the first 1000 hours of oxidation in 100% steam.

2 Experimental

2.1 Materials

The materials selected for the steam oxidation experiments are: T23, T347HFG. From these alloys curve (15 mm x 15 mm) and bridge (15 mm x 15 mm) shape specimens were machined (Figure 1). The wall thickness was 3 mm for T347HFG and 5 mm for T23. Before exposure samples were ground to a 600 grit surface finish and cleaned in volasil and then isopropanol in ultrasonic bath for ten minutes. The nominal chemical composition of materials tested is summarised in Table 1.

Alloy	C	Ni	Cr	Mo	W	Co	Mn	Fe	Si
T23	0.06	-	2.25	1.00	1.50	-	0.45	Bal	0.20
T347HFG	0.10	10.00	18.00	-	-	-	1.60	Bal	0.60

Table 1 Composition of the investigated alloys [wt. %]

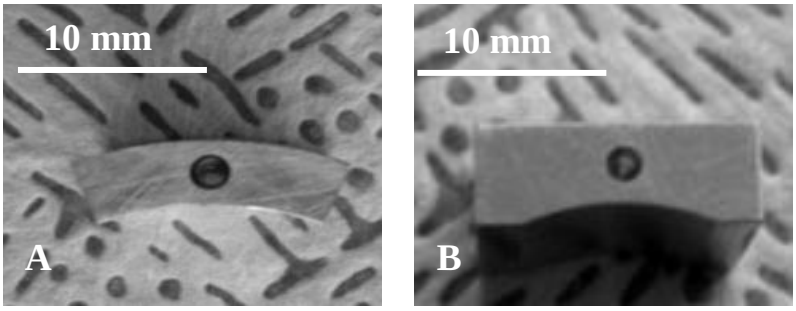

Figure 1 Specimen geometry: a - curve shape, b - bridge shape

2.2 Steam oxidation test

Steam oxidation tests were carried out in a horizontal furnace equipped with an alumina lined reaction tube (Figure 2). Samples were exposed to 100% steam environment for 1000 hours (four 250 hour cycles). The steam flow rate was set up for 12 l/h which equals velocity of 3.6, 3.8, 3.9 and 4.1 mm/s for 600 ^{o}C, 650 ^{o}C, 700 ^{o}C and 750 ^{o}C respectively. The scales formed on the alloys investigated were expected to exfoliate therefore the specimens were placed in the alumina crucibles to enable an overall mass change analysis and ensure a proper data collection, in particular at lower temperatures, when the mass change of the T347HFG is relatively low.

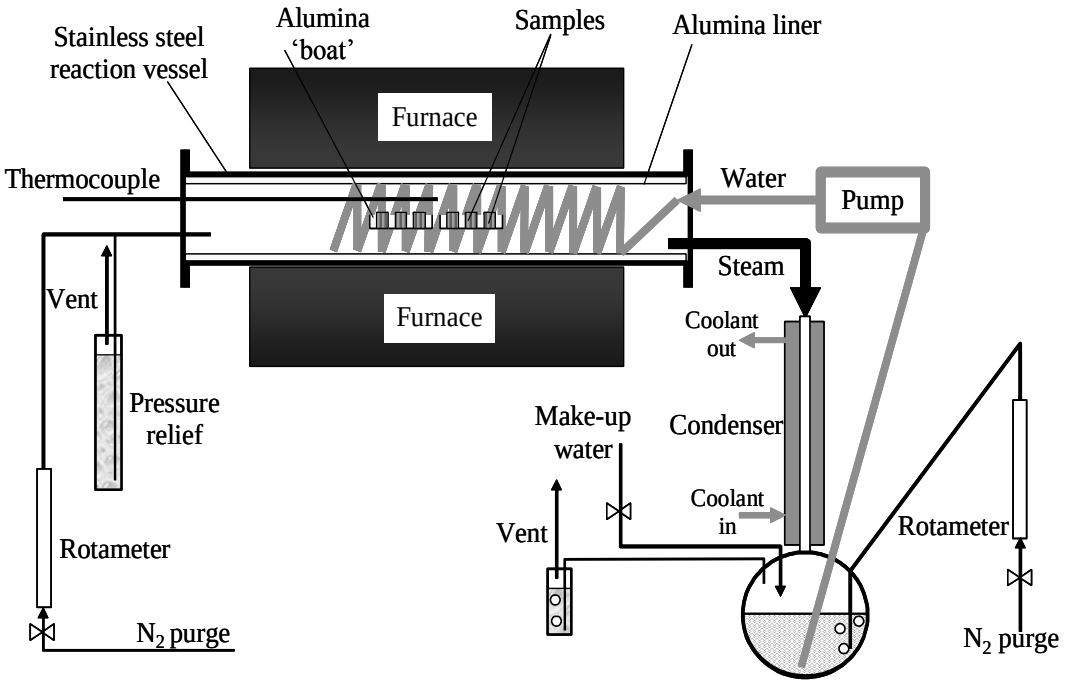

Figure 2 Schematic diagram of the steam oxidation tests' apparatus

In the steam oxidation test facility used, steam is generated by pumping water from a reservoir into the furnace and then the steam passes over the test samples and flows into a condenser before the water returns to the reservoir. The water used in the reservoir is double de-ionised. Before starting the test facility, the whole system is sealed and thoroughly purged using 'oxygen free nitrogen' (OFN). This purge continues through the water reservoir throughout the samples exposure period to minimise the level of oxygen in the system. The formed morphologies at high temperatures were characterisations after 250, 500 and 1000 hours exposure were obtained using Environmental Scanning Electron Microscopy (ESEM) coupled with Energy Dispersive X-ray (EDX) analyser. To investigate the mass change, the specimens were weighed using an analytical grade scale after each four 250 hours cycles. To do this, the samples were cooled down to room temperature in 100 % nitrogen atmosphere. Afterwards the crucibles with samples were placed in the chamber and heated up to the exposure the temperature: firstly in nitrogen to 100 ^{o}C, then up to the temperature of interest in 100 % steam.

3. Results

3.1 Kinetics

The isothermal experiments were carried at four temperatures: 600 ^{o}C - 750 ^{o}C. Figures 3 and 4 show the mass change for both analysed alloys during the 1000 hours test in steam environment and also show differences in mass change associated with the shape factor. Steam oxidation of T23 (2.25 wt%. of Cr) steel is faster than for T347HFG (18 wt% of Cr). Additionally the mass change of each alloy type varies with the sample geometry.

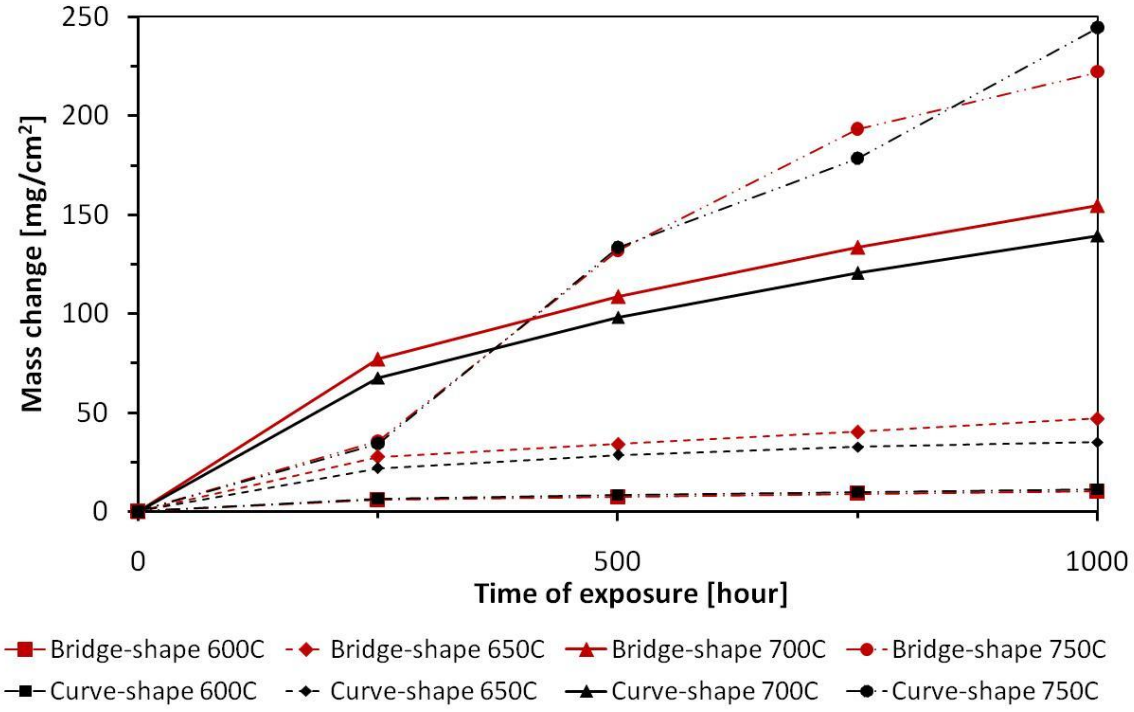

Figure 3 Comparison of mass change data for T23 alloy between 600 ^{o}C – 750 ^{o}C

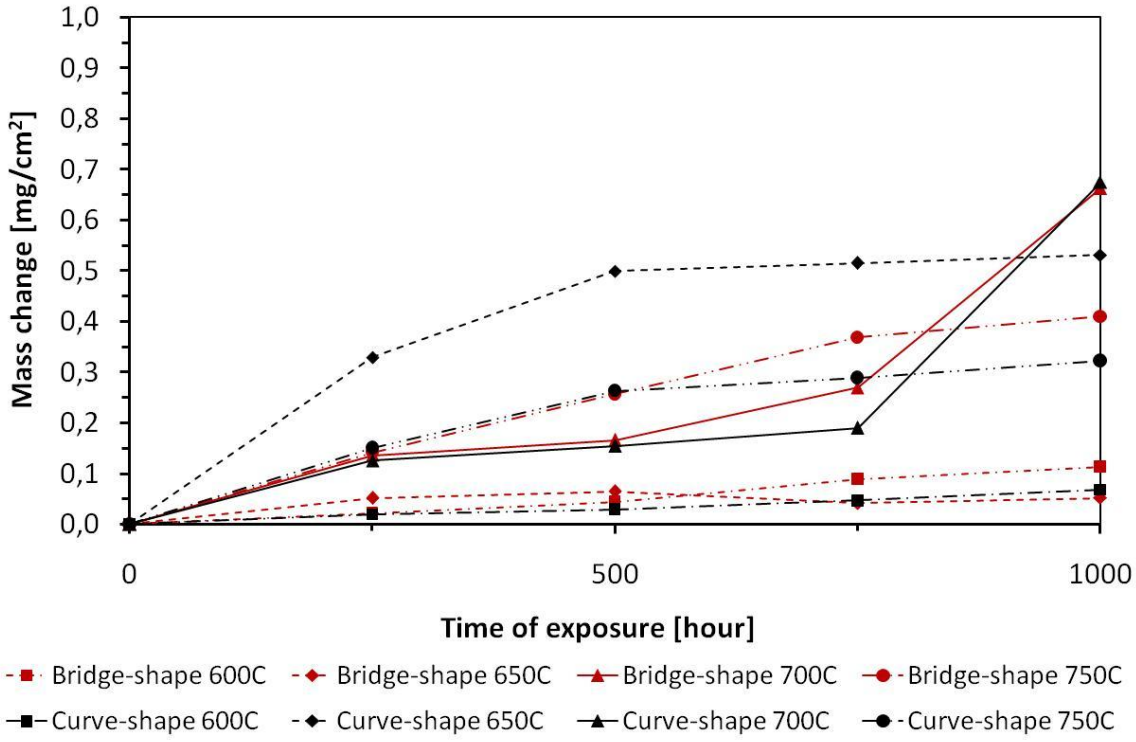

Figure 4 Comparison of mass change for T347HFG alloy between 600 ^{o}C – 750 ^{o}C

Figure 5 shows distribution of the mass change results for T23 at all analysed temperatures; the curves show that weight gain varies with specimens' geometry. The bridge shapes samples have larger mass change between 600 ^{o}C – 700 ^{o}C, however at 750 ^{o}C after 1000 hours exposure the curve shape specimen indicate larger mass change.

Figure 6 demonstrates that T347HFG alloy show even larger differences in mass gain with the shape factor. T347HFG alloy exposed at 600 ^{o}C, 700 ^{o}C and 750 ^{o}C indicates faster mass change for the bridge shape samples however at 650 ^{o}C the curve sample shows faster mass gain. Moreover the curve specimens show similar mass change at 650 ^{o}C and 750 ^{o}C.

In the case of bridge samples the mass changes significantly with temperature from 0.05 mg/cm^2 to 0.4 mg/cm^2 for 650 ^{o}C and 750 ^{o}C respectively. At 700 ^{o}C samples indicate the largest mass gain, which does not varies with sample geometries. To summarise T347HFG alloy oxidises in a slower manner, the mass gain is significantly lower (100 – 1000 times less than that observed in T23 alloy) with this difference being temperature dependent.

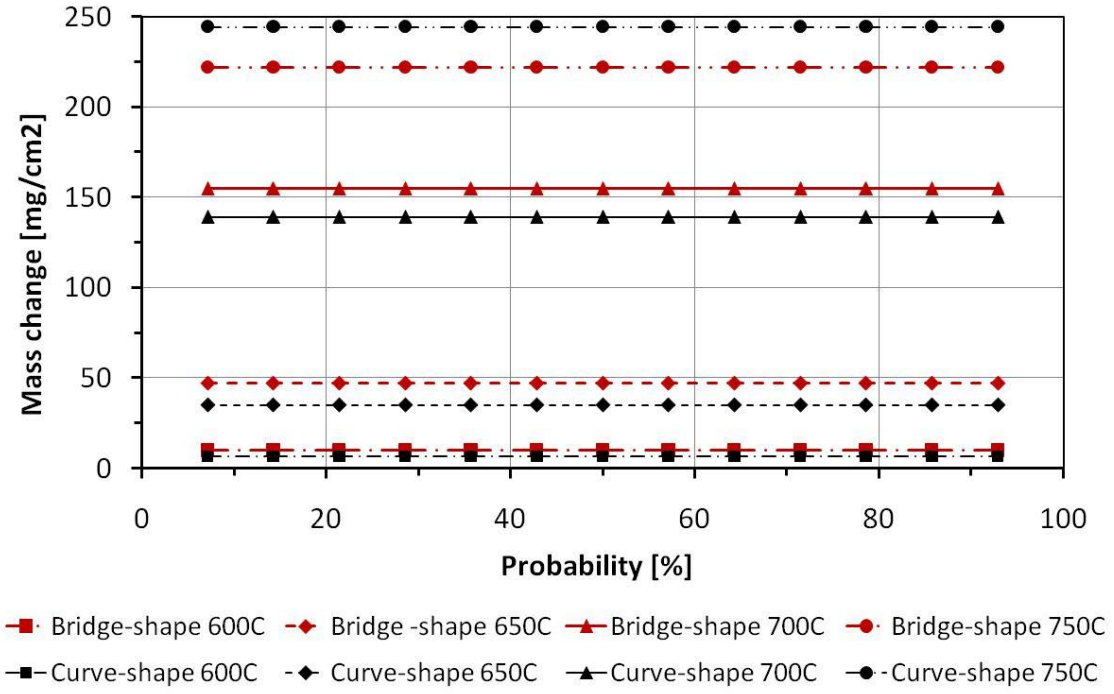

Figure 5 Distribution of mass change result for T23 alloy after 1000 hours exposure between 600 ^{o}C – 750 ^{o}C

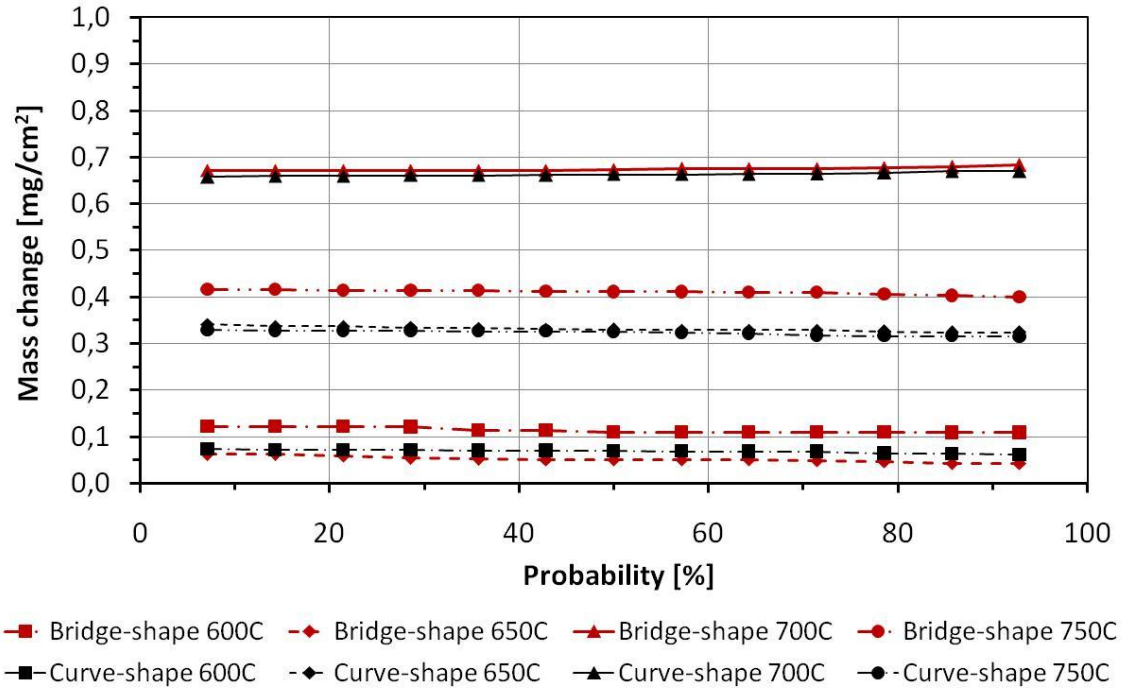

Figure 6 Distribution of mass change result for T347HFG alloy after 1000 hours exposure between 600 ^{o}C – 750 ^{o}C

3.2 Scale morphology

The morphology of the oxide scales developed on the alloys varies with temperature, specimen geometry and chromium content. Figure 7 (A-H) shows surfaces of the T23 and T347HFG alloys respectively. The surface of T23 steel at tested temperatures is covered with thick mixture of iron oxides. At 600 ^{o}C there is layer of hematite (Fe_2O_3) on the surface of the curve and bridge specimens; however magnetite (Fe_3O_4) is the main underlying oxide. With increasing temperature there is less Fe_2O_3 identified as the outermost layer as a results at 750 ^{o}C is lack Fe_2O_3 on the surface and the whole sample is covered with Fe_3O_4 (Figure 12G, H).

At both 600 ^{o}C and 650 ^{o}C the scale on T23 alloy starts to exfoliate due to the surface cracking through the outer oxide layers (Figures 7A and 10C). In comparison at 700 ^{o}C and 750 ^{o}C oxides layer are fully adherent to the surface, there is minimal exfoliation and the surface cracking (Figures 7E and 7G). XRD investigations performed on the exposed alloy at 700 ^{o}C indicated, that the surface is covered by the mixture of Fe_2O_3 and $Fe_{0.98}O$ (not shown here).

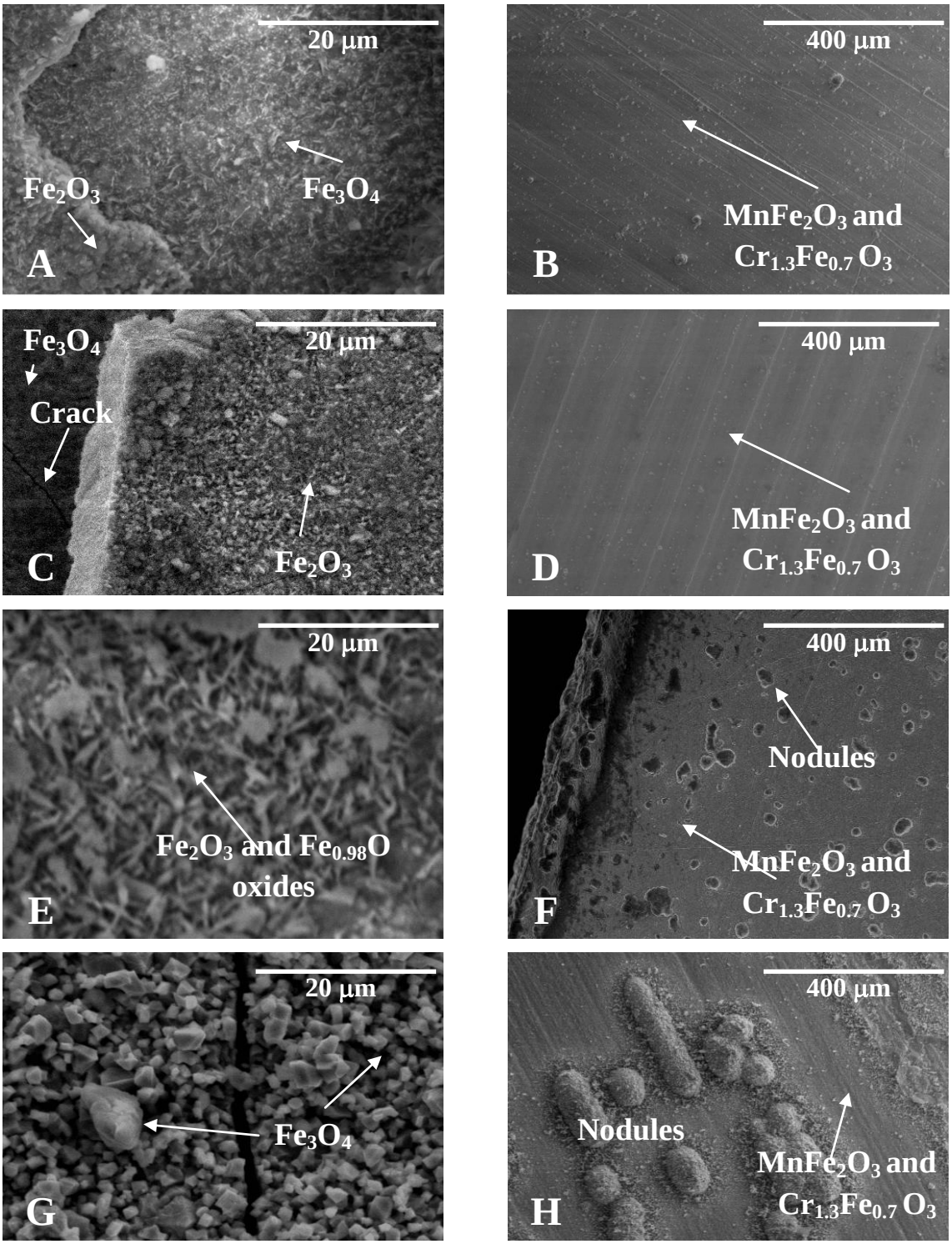

Figure 7 SEM pictures of oxidised surfaces after 1000 hours exposure: A, B– T23 and T347HFG at 600 ^{o}C; C, D – T23 and T347HFG at 650 ^{o}C; E, F – T23, T347HFG at 700 ^{o}C and G, H – T23 and T347HFG at 750 ^{o}C

T347HFG alloy at low temperatures (600 ^{o}C and 650 ^{o}C) thin layers of the protective oxides have developed, with thicknesses of few hundred nm (growing optical interference colours). Even at 750 ^{o}C after 1000 hours exposure T347HFG alloy is covered with a thin oxide scale (Figure 10H). However in regions there have been a local breakdown of the protective scale and the nodules (Figure 7H) have developed due to local imperilment of the protective oxides.

Nodules have also developed at 700 ^{o}C after 1000 hours exposure; however their size is significantly smaller (Figures 7E, G). At all temperatures studied the surface of T347HFG alloy is covered with thin protective oxides which were identified as mixture of chromium iron oxide ($Cr_{1.3}$ $Fe_{0.7}O_3$) and jacobsite ($MnFe_2O_4$) confirmed by XRD investigations (not shown here). Furthermore at higher temperatures the nodule of the fast growing oxides are formed (Figures 7F and 7H), their size is dependent on the exposure conditions.

T23 alloy oxidising in much faster manner than T347HGF alloy, therefore it develops much thicker and less protective oxide scales (Figure 8A-H). Even at the lower temperatures the scale is ≈ 70 μm thick. At 600 ^{o}C and 650 ^{o}C there are three layers can be distinguished; the inner layer with a mixed chromium and iron oxides as the main constituent is a M_3O_4 spinel, Fe_3O_4 is a middle and Fe_2O_3 as outer layer. The inner layer was adherent to the base material for the whole test duration at 600 ^{o}C for both curved and bridge-shaped specimens (Figures 8A and 8B). However at 650 ^{o}C it loses its adherence in case of the bridge shape sample next to the transition point between the flat and concave surface (Figure 8C); there is a gap formed after 1000 hours exposure between the alloy surface and the oxide scale, which most probably lead to scale exfoliation (Figure 9).

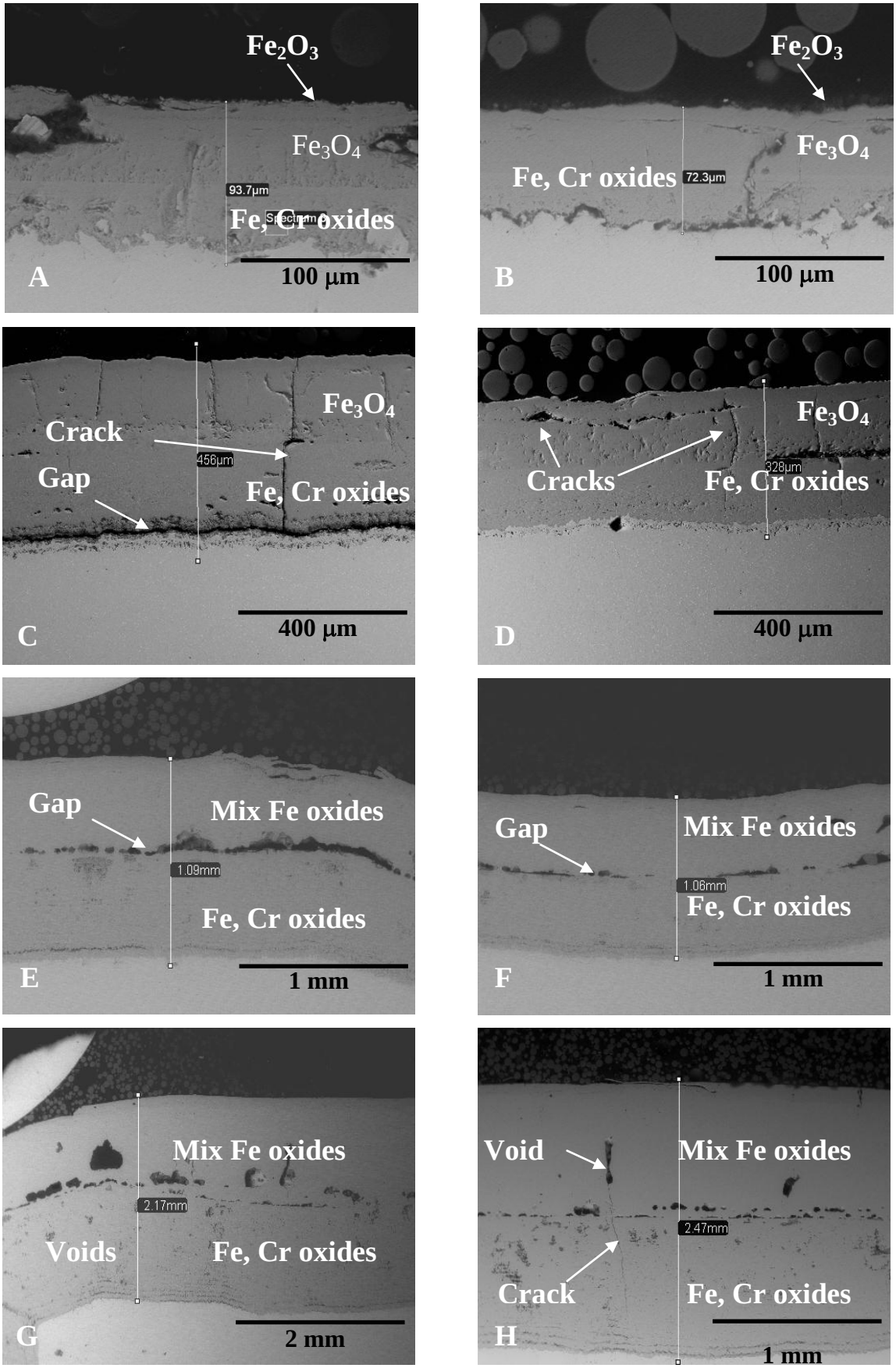

Figure 8 SEM picture of the scale developed on the T23 bridge and rectangular shape samples at 600 ^{o}C – A, B 650 ^{o}C – C, D 700 ^{o}C – E, F and 750 ^{o}C – G, H after 1000 hours exposure

The scale developed on the part of the bridge shape sample where the flat surface changes into concave, lost adherence after 1000 hours and started to exfoliate (Figure 9). The spallation was found above the interface between the inner and outer layer, where scale exhibits high level of stresses, due to transformation from flat to curve surface. Figure 8A and 8B show that at 600 ^{o}C the scale formed at T23 alloy is adherent, there are no significant amount of voids on flat surface of the bridge sample, however some were identified in the curve specimens and convex part of the bridge ones. There is no gap between the inner and outer layers at any point for both the analysed geometries.

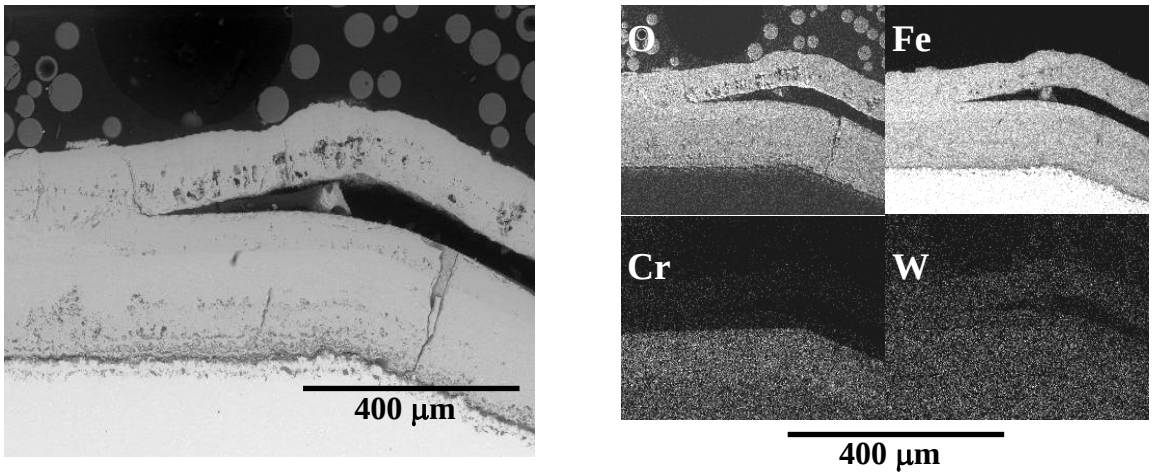

Figure 9 Mapping of the T23 bridge shape sample after 1000 hours exposure at 650 ^{o}C

The scale formed on T23 has low chromium content (Figure 9), the iron content changes with distance from the alloy surface. The delaminated part of the scale shows higher iron level than the inner part of the scale therefore conclusion that its main constituents are Fe_2O_3 and Fe_3O_4. In case of the curve shape samples there are no gaps (Figures 8D), the scale maintains the adherence for the entire test period, however it develops more cracks within and there are also a significant number of voids, which eventually will coalesce and finally due to the stress generated within the scale it will lose its adherence and exfoliate.

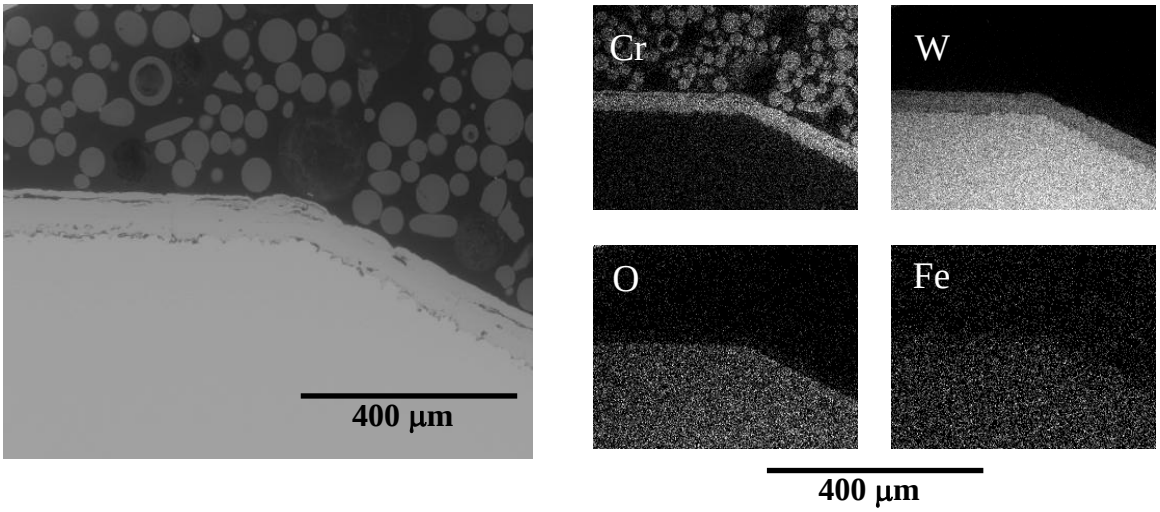

Figure 10 Mapping of the T23 bridge shape after 1000 hours exposure at 600 ^{o}C

EDX mapping analysis of the central layer at 600 ^{o}C (Figure 10) shows high concentration of iron oxide which has been identified as Fe_3O_4 while the outermost layer is Fe_2O_3 rich. Fe_2O_3 forms on the surface of Fe_3O_4, within which voids and cracks exist; thus there is more haematite on the surface of the bridge shaped samples. Figure 10 shows no exfoliation of the scale at 600 ^{o}C as it was seen in case of the sample exposed at 650 ^{o}C; however there is some gap formed in the interface between magnetite and haematite.

In contrast, steam oxidation of T23 alloy at 700 ^{o}C and 750 ^{o}C causes the development of thicker, multilayered inner scales, which are not protective but adherent. The multilayered structure has been identified by EDX as a mix of iron oxide, with Cr distribution within the layer differs substantially. More uniform distribution of the chromium within the multilayered inner scale at 750 ^{o}C was observed, whereas at 650 ^{o}C chromium content fluctuates. The outer layer was occupied by Fe_3O_4; there is not outermost layer of haematite as it was in case of samples exposed to steam at lower temperatures. At the interface between inner and outer layers voids have coalesced for both curved and bridge samples. The oxide scale developed on curved specimens is thicker than on flat part of the bridge shape whereas on the concave surface the oxides seem to be thicker and exhibit higher porosity. Moreover, next to the metal oxide interface the grain boundaries start to be visible due to voids injections, which has not been recognised in case of the curve specimens.

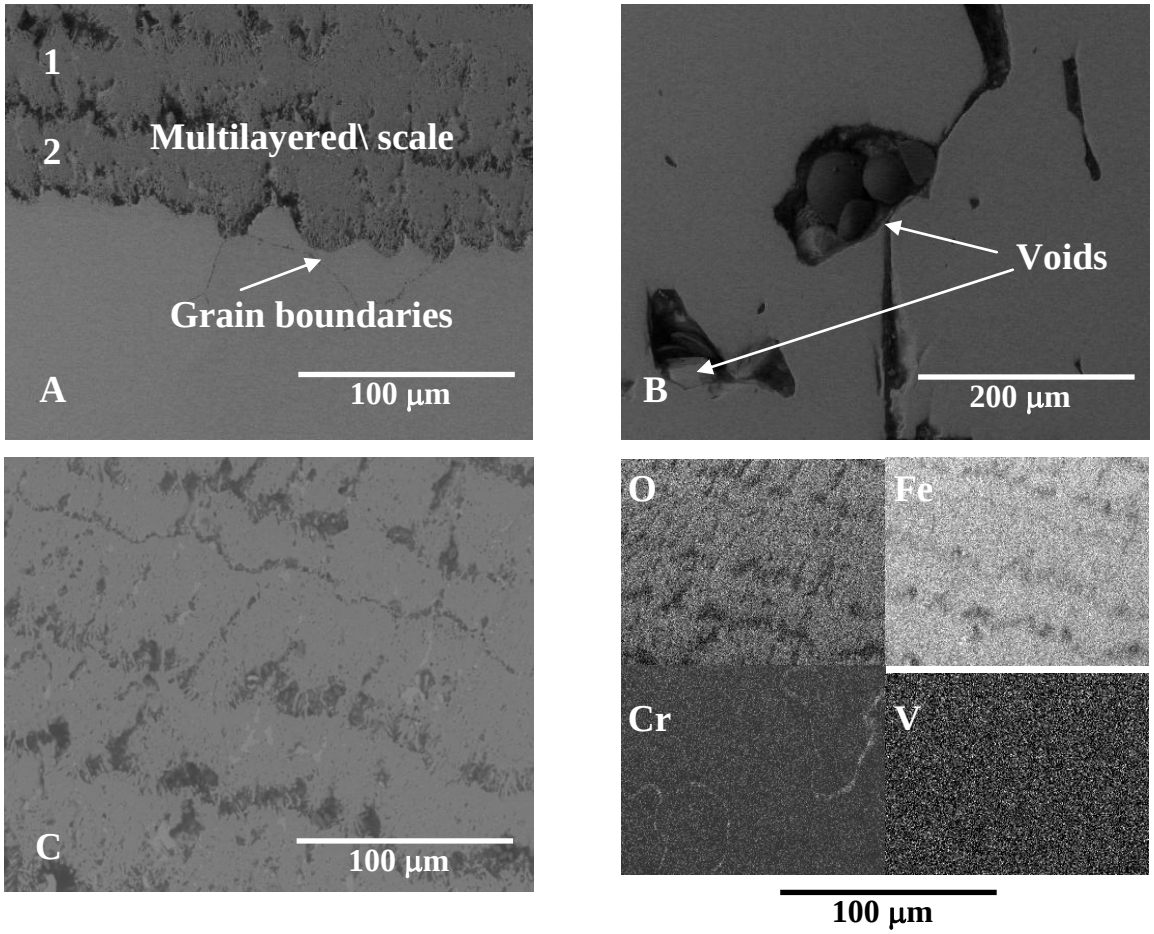

Figure 11 SEM picture of the T23 alloy after 1000 hours exposure at 750 ^{o}C A – multilayered inner structure, B – outer layer, C - Mapping of the multilayered inner scale formed on T23 bridge shape after 1000 hours exposure at 750 ^{o}C

The samples exposed at 750 ^{o}C exhibit cracks within the outer layers, as well as large voids (Figure 11B). Despite the significant number of cracks and voids within the layer it is still able to maintain adherence to the inner layer and there is no gaps nucleation between those parts of the scale during the 1000 hours exposure. Moreover, there are no gap at the alloy/scale interface unlike bridge shape specimens at 650 ^{o}C. T23 steel exposed to 700 ^{o}C does not exhibit large crack formation, however a gap has developed at the inner / outer layer interface.

In comparison, steam oxidation of T347HFG alloy leads to the formation of much thinner and more protective oxide scale than that observed on T23 (Figures 12A-F). T347HFG was covered with a protective mixture of chromium, iron oxide and jacobsite ($MnFe_2O_3$), the thickness of which differs with exposure temperature. There are some nodules on the sample surfaces. Figure 18F shows a nodule formed after 1000hours exposure at 750 ^{o}C; the EDX analysis (not shown here) indicate that it is a mixture of the Cr, Fe, Ni rich oxides Moreover the base material beneath the nodule oxidises internally (Figure 12D) which leads to iron oxide formation. The main constituents of the nodule are chromium, nickel and iron oxides. At lower temperature (600 ^{o}C and 650 ^{o}C) the scale consists of a non-uniform discontinuous layer (Figures 12A and 12B), however its discontinuity which spalls off during the cooling. Additionally there are no nodules identified on T347HFG samples after exposure at 600 ^{o}C and 650 ^{o}C.

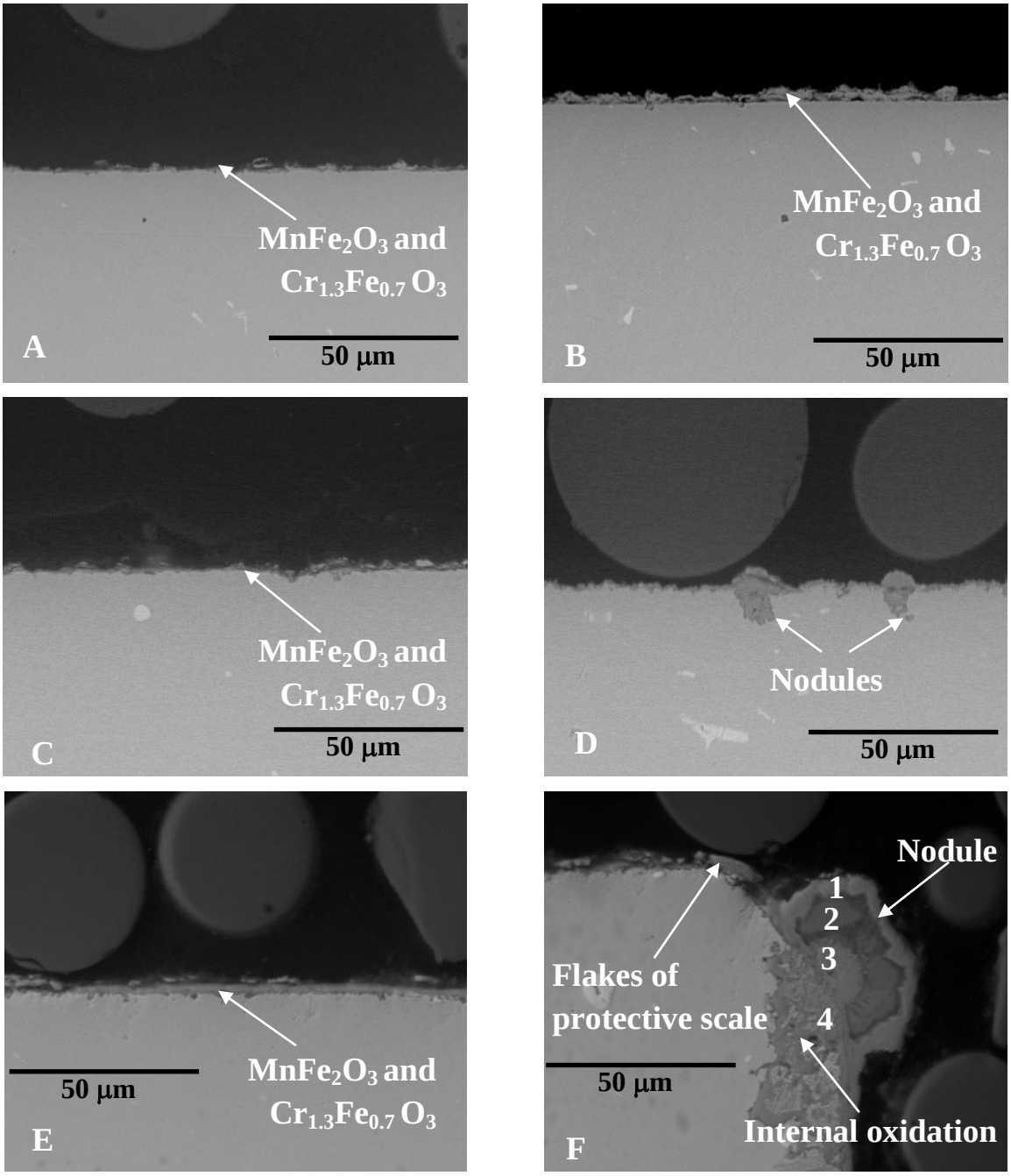

Figure 12 SEM pictures of the 347HFG after 1000hours exposure A -thin oxides layer formed at 600 ^{o}C, B – thin - discontinuous chromia scale at 650 ^{o}C, C - protective chromia scale at 700 ^{o}C, D – nodule at 700 ^{o}C E– continuous protective chromia scale at 750 ^{o}C, F – nodule at 750 ^{o}C

To summarise ferritic T23 steel exhibits fast oxidation rate at all temperatures, and leads to the development of the thick non protective oxide scale. The formed scale is double or triple-layered with an inner iron/chromium spinel under a magnetite layer, in addition between 600 ^{o}C – 700 ^{o}C there is additional haematite as the outermost layer. Above 700 ^{o}C the scale morphology changes, the outer scale is occupied by magnetite, lack of Fe_2O_3 has formed, the inner layer becomes multilayered, it has been identified as the wustite (FeO) and (Fe, Cr) spinel. The multilayered inner oxides formed due to the higher exposure temperature of the material which enables FeO formation.

In contrast T347HFG shows slow oxidation rates in the tested temperature range. At 700 and 750 ^{o}C there are nodules forming on the surface as a result of the breakdown of the protective oxides. Size of which varies with the exposure conditions and time. The higher level of the chromium (18%) in this material results in formation of the mixed chromium iron oxide and jacobsite. The protective scale is developed across the whole temperature range examined, however at 700 ^{o}C and 750 ^{o}C the scale becomes more adherent and continuous and therefore more protective than at lower temperatures. At 600 ^{o}C and 650 ^{o}C the scale examined is not continuous and non adherent as a result exfoliation during cooling process. At 700 ^{o}C and 750 ^{o}C there are some local breakdowns of the protective oxide which have driven nodule formation.

4. Discussion

In terms of mass change data, steam oxidation of the investigated T23 (2.25 wt. % of Cr) steel follows a parabolic rate dependence. However, it shows an initial deviation from this [19]. Zurek et al. [20] believes that the initial oxidation of low Cr ferritic steels follows a linear rate law as result of the fast oxidation of the oxide free alloy surface, but as soon as the newly formed layer thickens the dependence transforms to parabolic. Despite the transformation of rates being well recognised, the identification of the exact transformation point is complicated [7]. In case of the tests conducted, it varies with the temperature, possibly a result of changes in element diffusion rates with temperature and therefore faster breakaway oxidation of the protective thin oxides formed on the bare alloy's surface. This is in agreement with findings of Ennis and Quadakkers [5], who believe that the transformation point between the rates is associated with fact that the initial period of oxidation under different exposure condition may last from a few seconds to hundreds of hours.

Oxidation of T23 at investigated temperatures seems to follow the parabolic law however above 650 ^{o}C the process significantly accelerates most probably due to the FeO formation, after longer exposure it could transform to linear. This is in accordance with Wright and Pint [21], who concluded that at temperatures above 600 ^{o}C – 650 ^{o}C steam oxidation rate is closer to linear. It is also confirmed by Lepingle et al. [22] that the oxidation of T23 starts to exhibit dependence close to linear above 650 ^{o}C. Result of the tests in this study show that steam oxidation in temperature range 600 ^{o}C – 750 ^{o}C shows the parabolic rate dependence (750 ^{o}C) the oxidation rate follows. At 600 ^{o}C the oxidation of T23 is much slower; Komai et al. [23] and Lepingle et al. [22] believed that it follows the parabolic behaviour.

The activation energy for T23 at analysed temperatures was calculated for -335 kJ/mol which is in good agreement with Fry et al. [24]. In contrast Wright and Dooley [9] have calculated the activation energy in the temperature range between 500 ^{o}C – 700 ^{o}C as being -230 kJ/mol, however that value was based on the number of independent test performed by different groups of researchers. The discrepancy of results is most probably caused due to diverse test conditions, experimental procedures and the analytical approached to the data obtained. According to Patterson et al. [25], a change in steam pressure to which the material is exposed results in thicker scale formation which means that the oxidation rates are faster and therefore the values of the activation energy differ. There are number of the variables such as steam flow, water chemistry which may also influence the results [13].

The tests conducted showed slower oxidation rate for T347HFG alloy at temperatures of interest, this is associated with its higher chromium content and therefore formation of more protective oxides which significantly slow down the oxidation process [7]. There are only limited published data for the oxidation kinetics of T347HFG at temperature range of this in 1 bar steam [7]. Wright et al. [9] show that even after longer exposure at high temperatures the T347HFG shows slower oxidation. The mass gains of the T347HFG are 20, 63 and 91 mg/cm^2 after 40kh exposure at 600 ^{o}C, 650 ^{o}C and 675 ^{o}C respectively [9]. Moreover work of Hansson and Montgomery [6] confirmed oxidation of this type of alloy to be slow; with the oxide scale of T347HFG exposed at 625 ^{o}C after over 7000 hours being still less than 1 μm thick, which correspond to slow oxidation rates. Analysis of the oxidation kinetics of T347HFG shows that oxide growth rate do not follow fully the parabolic rate law, therefore it is assumed to be sub-parabolic. In contrast Wright and Dooley [9] believed that the oxidation of the T347HFG at high temperature follows closely the parabolic rate law. This is also in agreement with Viswanathan et al. [7] and Saunders and McCartney [26]. Activation energies derived from the data obtained (Table 2) are in agreement with Fry et al. [24], who give a value of energy for -132 kJ/mol. The differences in activation energies values are most probably due to different samples treatment, exposure conditions and procedures [13].

As it was presented in the result section, the scale developed on T23 at 600 ^{o}C and 650 ^{o}C double-layered with local growth of third outermost layer of haematite, in agreement with Otsuka et. al [15] and Nishimura et al. [27]. Moreover Lepingle et al. [22] and Komai et al. [23] indicated that the scale consist of two types of oxides; the inner layer is rich in the $(Fe,Cr)_3O_4$ spinel, whereas the main constituent of the outer layer is magnetite, additionally there are some traces of the haematite identified as the outermost layer [2, 7 , 9]. In particular tests the haematite has formed between 600 ^{o}C, and 700 ^{o}C; there is no track of it at 750 ^{o}C. Fe_2O_3 forms on the surface of T23 samples at the beginning of the process most probably due to the relatively high oxygen partial pressure as the result of the slower iron diffusion from the metal to the magnetite, which is caused by the existence of the Cr rich spinel [23]. After longer exposure, when the protective properties of the Fe-Cr spinel are lower due to fact that T23 alloy is not able to sustain the protective layer (low Cr content in the base material) haematite forms above the region with large amount of voids and cracks which significantly reduce the iron diffusion [27]. At higher temperatures (700 ^{o}C -750 ^{o}C) a multilayered inner scale forms. According to Wright and Dooley [9] this structure consists of the repeating double series of the Fe-Cr spinel, however the result of the EDX analysis show also

significant content of the iron which corresponds to magnetite, therefore the conclusion is that the multilayered structure is mix of the Fe-Cr spinel and Fe_3O_4 [8] (Figure 18C).

Some authors report a multilayered inner structure forming as a result of heat flux [8, 9], the heat flux is reported by Osgerby and Quadakkers [13] to be the major difference between laboratory exposure procedures and plant conditions. Griess et al. [28] have shown that even at higher temperature in laboratory test the oxidation rates and scale changes are slower than in the exposures where the heat flux is present. However the existence of multilayered oxides maybe explained by higher exposure temperatures [8]. Under such condition wustite (FeO) is able to form, when the scale cools down the wustite layer decomposes to magnetite and in many cases transforms to duplex layer of magnetite or mixed Fe_3O_4 and Fe-Cr spinel [8]. From the power plant experience point of view the development of the multilayered inner structure is explained as a result of steam flow rates causing faster oxide growth.

The double-layered oxide scale is present of both types of the specimen geometries; however its thickness differs. The oxides developed on the bridge shape specimens are thicker for both 600 ^oC and 650 ^oC. The scale is the thickest on the concave and flat surfaces of the specimen, the scale is thinner where flat surface transform to concave. This is associated with stress development which causes scale exfoliation; the scale growing there will be under higher stress therefore there is greater probability of the scale spallation [29]. Additionally at temperature of 650 ^oC there is substantial amount of haematite growing on that part of the scale which will again leads to exfoliation due to differences in coefficients of thermal expansion (CTE) between Fe_2O_3 and Fe_3O_4 [17]. The stress generated upon sample cooling is tensile, moreover according to Otsuka et al. [15] the exfoliation is affected by the radial stress, which leads to spallation if is larger than adhesion strength of the oxide scale. During the exposure of bridge samples the gaps nucleate at the inner/outer scale interface, within the oxides at the concave surface and at the transition between the flat and concave surfaces; however they heal after longer exposure times. The healing may be explained by access of oxygen molecules through magnetite and haematite [17]; instead there is gap between metal and oxide scale. On the other hand there are more voids and a gap present at the interface between inner and outer scale of the curve samples which results in the haematite formation [27]. The amount of hematite on the surface of the analysed samples was also dependent on the sample position within the furnace. The part of the samples facing steam flow develops more Fe_2O_3.

Moreover there are small differences in the temperature distribution within the hot zone, which could have an impact on the haematite formation in the regions with higher temperature. Furthermore the amount of haematite is larger on the curve and the concave part of the bridge-shape specimens, where voids and gaps have formed. In contrast the surface which is at the counter-position to steam flow shows less haematite and spallation.

The scales formed on the T347HFG analysed are significantly thinner than those on T23; this is result of the formation of protective oxide [21]. According to Viswanathan et al. [7] the scale formed on austenitic steels is 2 - 3 times thinner than on ferritics; however for these particular tests the difference is more significant. The better resistance of the T347HFG is not just associated with higher chromium content (18%) but also with the grain structure [6, 9]. The fine grain structure of T347HFG significantly increases the of the Cr supply to the protective oxides by grain boundary diffusion and so the thin chromia scale can last longer. Hansson and Montgomery [6] reported that even after over 7000 hours exposure at 625 ^{o}C the alloy is covered with thin around 1 μm layer of Cr_2O_3. Additionally they show that the uniform layer of chromia is able to form after 500 hours 700 ^{o}C and suppress the un-protective oxide growth up to 2000 hours. For particular tests a thin layer of $Cr_{1.3}$ $Fe_{0.7}O_3$ and $MnFe_2O_4$ has formed after exposure at all temperatures tested, however its thickness varies with exposure conditions. The fast development of the protective oxides scale above 700 ^{o}C is due to enhanced chromium diffusion in the grain boundaries [6]. After longer exposure at 700 ^{o}C and 750 ^{o}C the protective scale breaks down and double-layered nodules start to nucleate on the surface. The protective oxide scale formed on T347HFG is able to prevent fast nodular growth; however, eventually after longer exposures the double-layered scale will spread along the surface [9]. The double-layered nodule consists of iron oxide with some traces of chromium and nickel, whereas the inner part is the mix of Fe-Cr spinel and magnetite. The formation of the nodules is explained by the penetration of the protective scale along the grain boundaries, furthermore due to the outward diffusion of chromium the chromium-depleted boundaries are able to oxidise to magnetite. Moreover development of the nodular oxides is influenced by surface defects, additionally the number of nodules increases in the corners and on the edges of the samples, which is associated with grain orientation and higher stresses within the material.

After longer exposure the surfaces of T347HFG forms a double-layered scale , which at temperature between 575 ^{o}C – 650 ^{o}C and 1 bar steam consists of outer layer with magnetite as the main constituent and the inner structure of Fe-Cr spinel [9]. This is in agreement with findings from Hansson and Montgomery [6]. However Hughes et al. [30]

have shown that at 670 ^{o}C after 11000 hours a double layer forms, where the outer layer is mix of Fe_2O_3 and Fe_3O_4 whereas the inner layer consist of Cr_2O_3.

To summarise the oxidation of T347HFG is significantly slower than T23 due to formation of an adherent and protective mixture of chromium/iron oxide and jacobsite on the surface of the alloy, which is a good diffusion barrier [9]. Such protection significantly slows down the oxidation rates, as well as, the development of less protective oxides such as Fe-Cr spinel or iron oxides [6] T23 alloy contains a relatively low amount of chromium which does not allow it to form a continues chromia layer [16]; therefore the oxidation is significantly faster as the Cr-Fe spinel is less protective [7]. The analysis of the steels performance in steam oxidation at 600 ^{o}C, 650 ^{o}C, 700 ^{o}C and 750 ^{o}C show that T23 is not a good candidate for boilers components operating at any of these temperatures [10], whereas the T347HFG could be successfully used. However in practice other properties especially creep also limit the use of these alloys.

5. Conclusions

Steam oxidation performance of the T23 and T347HFG alloys at 600 ^{o}C, 650 ^{o}C, 700 ^{o}C and 700 ^{o}C with special consideration of the specimen geometry were analysed and discussed. Based on obtained results from the 1000 hours isothermal tests conducted following conclusions are drawn.

1. T23 (2.25 wt% of Cr) steels exhibits much fast mass change at all tested temperatures, which corresponds with fast oxide growth and low concentration of Cr;
2. There is a clear impact of the specimen geometry on the mass change of the T23 samples, the samples with more complex geometries indicates larger mass change, and it seems to have an impact on the development of the haematite on the surface of the magnetite due to generation of voids;
3. At higher temperatures, T23 develops a multilayered inner scales structure, which is identified as the mixture of the iron and chromium oxides;
4. T347HFG (18.0 wt% of Cr) shows good steam oxidation resistance in the conditions tested, which is associated with formation of the protective oxide scale
5. Oxidation of T347HFG leads to formation of the double-layered nodules in the regions with breakaway of the protective scale.

Acknowledgments

We would like to acknowledge the support of The Energy Programme, which is a Research Councils UK cross council initiative led by EPSRC and contributed to by ESRC, NERC, BBSRC and STFC, and specifically the Supergen initiative (Grants GRyS86334y01 and EPyF029748) and the following companies; Alstom Power Ltd., Doosan Babcock, E.ON, National Physical Laboratory, Praxair Surface Technologies Ltd, QinetiQ, Rolls-Royce plc, RWE npower, Siemens Industrial Turbomachinery Ltd. and Tata Steel, for their valuable contributions to the project.

References

[1] S.J Sandler, **1999**, Chemical and Engineering Thermodynamics, 3rd edition, Wiley, New York, USA

[2] R. Viswanathan, W.T. Bakker, **2000**, Materials for Boilers in Ultra Supercritical Power Plants.. Miami Beach : ASME, 2000 International Joint Power Conference. (), 2-22

[3] D.J. Young, **2008**, High Temperature Oxidation and Corrosion of Metals. Vol. 1 Elsevier, Amsterdam, The Netherlands

[4] P.J. Ennis, W. J. Quadakkers, **2007**, Implications of steam oxidation for service life of the high- strength martensitic steel components in high-temperature plant, International Journal of Pressure Vessels and Piping, 82-87.

[5] P.J. Ennis, W.J. Quadakkers, **2007**, Mechanisms of steam oxidation in high strength martensitic steels, International Journal of Pressure Vessels and Piping, 75-81.

[6] A.N. Hansson, M. Montgomery, Long term Steam Oxidation of TP 347H FG in Power Plant, **2006**, Materials Science Forum, 22(3-4):263-2670.

[7] R. Viswanathan, J. Sarver, J. M. Tanzosh, **2005**, Boiler Materials for Ultra-Supercritical Coal Power Plants - Steamside Oxidation, Journal of Materials Engineering and Performance, 15, 255-274

[8] Electric Power Research Institute . Program on Technology Innovation **2007**: Oxide Growth and Exfoliation on Alloys Exposed to Steam, EPRI Report

[9] I. G. Wright, R. B. Dooley, **2010**, A review of the oxidation behaviour of structural alloys in steam. International Materials Reviews. 129-167

[10] I. G. Wright, P. J. Maziasz, F. V. Ellis, T. B. Gibbons, D. A. Woodford, **2004**, Materials Issues for turbines for operation in ultra-supercritical steam. Clearwaters, 29th International Technical Conference on Coal Utilization and fuel systems.

[11] R. Viswanathan, R.Purgert, U. Rao, **2002**, Materials technology for advance coal power plants, EPRI Report

[12] J. Gabrel, C. Coussement, L. Verelst, R. Blum, Q Chen, C. Testani, **2001** Superheater Materials Testing for USC Boilers: Steam Side Oxidation Rate of (Advanced Materials in Industrial Conditions. Materials Science Forum, 369-372.

[13] S Osgerby, J Quadakkers, **2005**, The influence of laboratory test procedures on scale growth kinetics and microstructure during steam oxidation testing. Materials at High Temperatures, 22, 27-33

[14] L. Sanchez, M. P. Hierro, F. J. Perez, **2009**, Effect of Chromium Content on the Oxidation Behaviour of Ferritic Steels for Applications in steam atmospheres at high temperatures, Oxidation of Metal, 71, 3-4, 173-186

[15] N. Otsuka**,** **2005**, Fracture behaviour of the steam-grown oxide scales formed on 2 - 12%Cr steels. Materials at high temperatures, 22(1-2):131-138.

[16] A. Shibili, F Star, **2007**, Some aspects of plant and research experience in the use of new high strength martensitic steel P91. Pressure Vessels and Piping. 84, 1-2, 114-122

[17] W. Quadakkers, P. Ennis, J. Żurek, M. Michalik, **2005**, Steam oxidation of ferritic steels - laboratory test kinetics data, Materials at High Temperatures, 22, 1-2 47-60

[18] J. Ehlers, D. J. Young, E. J. Smaardijk, A. K. Tyagi, H. J. Penkalla, L. Singheiser, W. J. Quadakkers, **2006** Enhanced oxidation of the 9% Cr steel P91 in water vapour containing environments, Corrosion Science, 48, 11, 3428-3454

[19] K. Natesan, J. H. Park, **2007** Fireside and Steamside corrosion of alloys for USC plants, International Journal of Hydrogen Energy, 32, 16, 3689-367

[20] J. Żurek, E. Wessel, L. Niewolak, F. Schmitz, T. U. Kern, L. Singheiser, W. J. Quadakkers, Anomalous temperature dependence of oxidation kinetics during steam oxidation of ferritic steels in the temperature range 550 - 650 ^{o}C, Corrosion Science (2004), 2301-2317

[21] I.G. Wright, B. A. Pint, An assessment of the high-temperature oxidation behaviour of Fe-Cr steels in water vapour and steam **2002** Denver, USA NACE CORROSION

[22] V. Lepingle, G. Louis, D. Petelot, B. Lefebvre, J Vaillant 2001, High temperature corrosion behaviour of some boiler steels in pure water vapour. Materials Science Forum, 369-372, 239-246.

[23] N. Komai, F. Masuyama, M. Igarashi, **2005**, 10-Year Experience with T23 (2.25Cr-1.6W) and T122 (12Cr-0.4Mo-2W) in a Power Boiler, Journal of Pressure Vessel Technology 127

[24] A. Fry, S. Osgerby, M. Wright **2002**, Oxidation of Alloys in Steam Environments - A Review. Teddington : National Physical Laboratory, UK

[25] S. R. Paterson, R. Mosser, T. Rettig, **1992,** Integration of iron-based materials with water and steam. Heidelberg: EPRI Report, USA

[26] S. R. J. Saunders, L. N. McCartney, **2006** Current understanding of steam oxidation - power plant and laboratory experience, Materials Science Forum, 522 – 523, 119-128.

[27] Nishimura, N. Komai, Y. Hirayama, F Masuyama, **2005**, Japanese experience with steam oxidation of advanced heat-resistant steel tubes in power boilers, Materials at high temperatures, 3-10.

[28] J.C. Griess, J. H. Devan, W. A. Maxwell, Long term corrosion of Cr-Mo steels in superheated steam at 482 and 538 ^{o}C **1982** Material Performance 18 – 24

[29] I.G. Wright, M. Schutze, S. R. Paterson, P. F. Tortorelli, R. B. Dooley, **2004**, Progress in prediction and control of scale exfoliation on superheater and reheater alloys. San Diego: EPRI Report.

[30] A H. Ughes, R. B. Dooley, S. Paterson, **2003**, Oxide exfoliation of 347HFG in high-temperature boilers, Sydney : Institute of Materials Engineering Australasia Ltd,.